

Supplementary Material

SARS-CoV-2 infection in the central nervous system of a 1-year-old infant submitted to complete autopsy

Ismael Gomes^{1,3*}, Karina Karmirian^{2,3*}, Júlia T. Oliveira^{2*}, Carolina da S. G. Pedrosa^{2*}, Fernando Colonna Rosman^{1,5}, Leila Chimelli⁴, Stevens Rehen^{2,3}

*These authors contributed equally to this work

Corresponding authors:

Stevens Rehen (srehen@lance-ufrj.org)

Leila Chimelli (chimelli@hucff.ufrj.br)

Affiliation details:

1 - Anatomic Pathology Service, Jesus Municipal Hospital, Rio de Janeiro, RJ, Brazil.

2 – D’Or Institute for Research and Education (IDOR), Rio de Janeiro, Brazil.

3 – Institute of Biomedical Sciences, Federal University of Rio de Janeiro (UFRJ), Rio de Janeiro, Brazil.

4 - Laboratory of Neuropathology, State Institute of Brain Paulo Niemeyer, Rio de Janeiro, RJ, Brazil. Post-Graduate Programs of Pathology and Translational Neuroscience, UFRJ,

5 - Department of Pathology, School of Medicine, UFRJ, Rio de Janeiro, Brazil.

Supplementary Methods

Immunofluorescence

Paraffin blocks from lungs and brain (choroid plexus [ChP], cerebral cortex, globus pallidus, lateral ventricle, medulla oblongata, midbrain, pons and putamen) were selected to produce a tissue microarray, as adapted from Pires et al. (2006) (7). Four μm sections were deparaffinized, rehydrated, followed by 10 mM citrate buffer (pH 6.0) antigen retrieval for 30 minutes at 98°C and blocked/permeabilized (3% bovine serum albumin/0.3% Triton X-100). Overnight incubation at 4°C was performed with anti-SARS-CoV-2 spike protein monoclonal antibody (SP), GTX632604, 1:500. Then, the slides were washed with PBS and incubated with secondary antibody (Goat anti-Mouse Alexa Fluor 488, 1:400; A-11001) for 45 minutes at 37°C. Nuclei were stained with 0.5 $\mu\text{g}/\text{mL}$ 4'-6-diamino-2-phenylindole for 5 minutes and the slides were mounted with Aqua-Poly-mount (Polysciences). Images were acquired with a confocal microscope Leica TCS SP8 using a 63x objective lens.

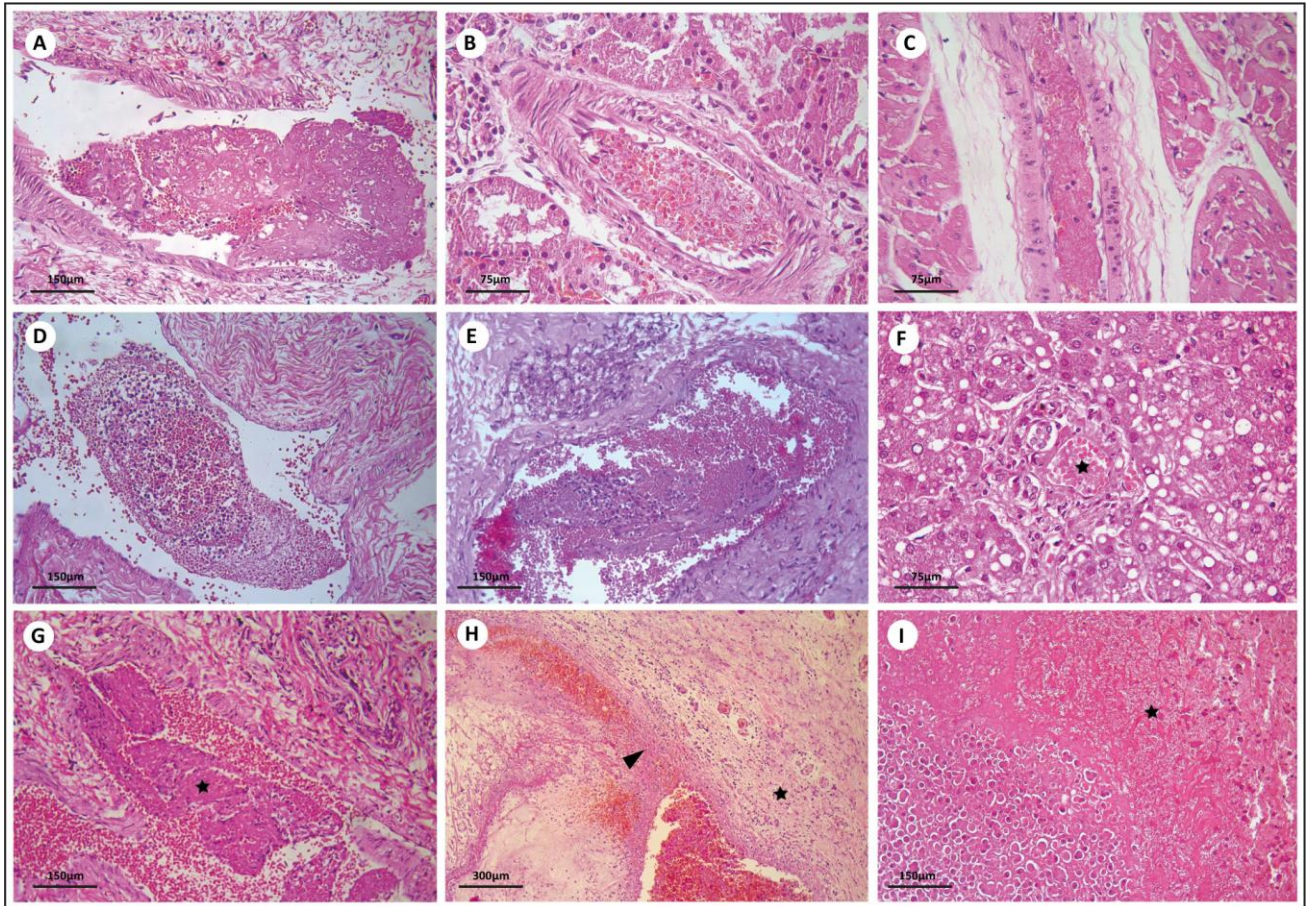
Immunohistochemistry

From selected areas of the nervous tissue which presented histological lesions, immunohistochemical reactions were performed, using the following monoclonal antibodies (Cell Marque, Sigma-Aldrich Co, Rocklin, CA, USA) and dilutions: anti-gliial fibrillary acidic protein- GFAP-clone EP672y, (1:500), anti-NeuN (Zeta Corporation, Arcadia, CA, USA) Clone A100 (1:200), CD3 (Clone MRQ-39), and CD68 (Clone Kp-1), according to standard protocols. Five μm thick tissue sections were incubated in a drying oven at 37 °C for six hours and then deparaffinized in xylene. The tissue sections were rehydrated by placing in decreasing concentrations of alcohol and washed in distilled water. To enhance antigen retrieval, the tissue sections were pretreated in an Electric Pressure cooker for 15 minutes in the solution 1:20 Declere® (pH 6) / 1:100 Trilogy (pH9) in distilled water. To block endogenous peroxidase activity, the tissue sections were exposed to hydrogen peroxide, washed with distilled water and rinsed in phosphate buffered saline (PBS) to stop enzymatic digestion. They were then incubated with the primary antibody overnight at 4°C, rinsed in PBS for 5 minutes and incubated with Polymer Hi Def (horseradish peroxidase system) for 10 minutes at room temperature preceded by several washes in PBS. The peroxidase reaction was visualized with DAB substrate, rinsed in running water; the sections were then counterstained with Meyer's hematoxylin for 1 minute, washed in running tap water for 3 minutes, dehydrated in alcohol, cleared in xylene and mounted in resinous medium.

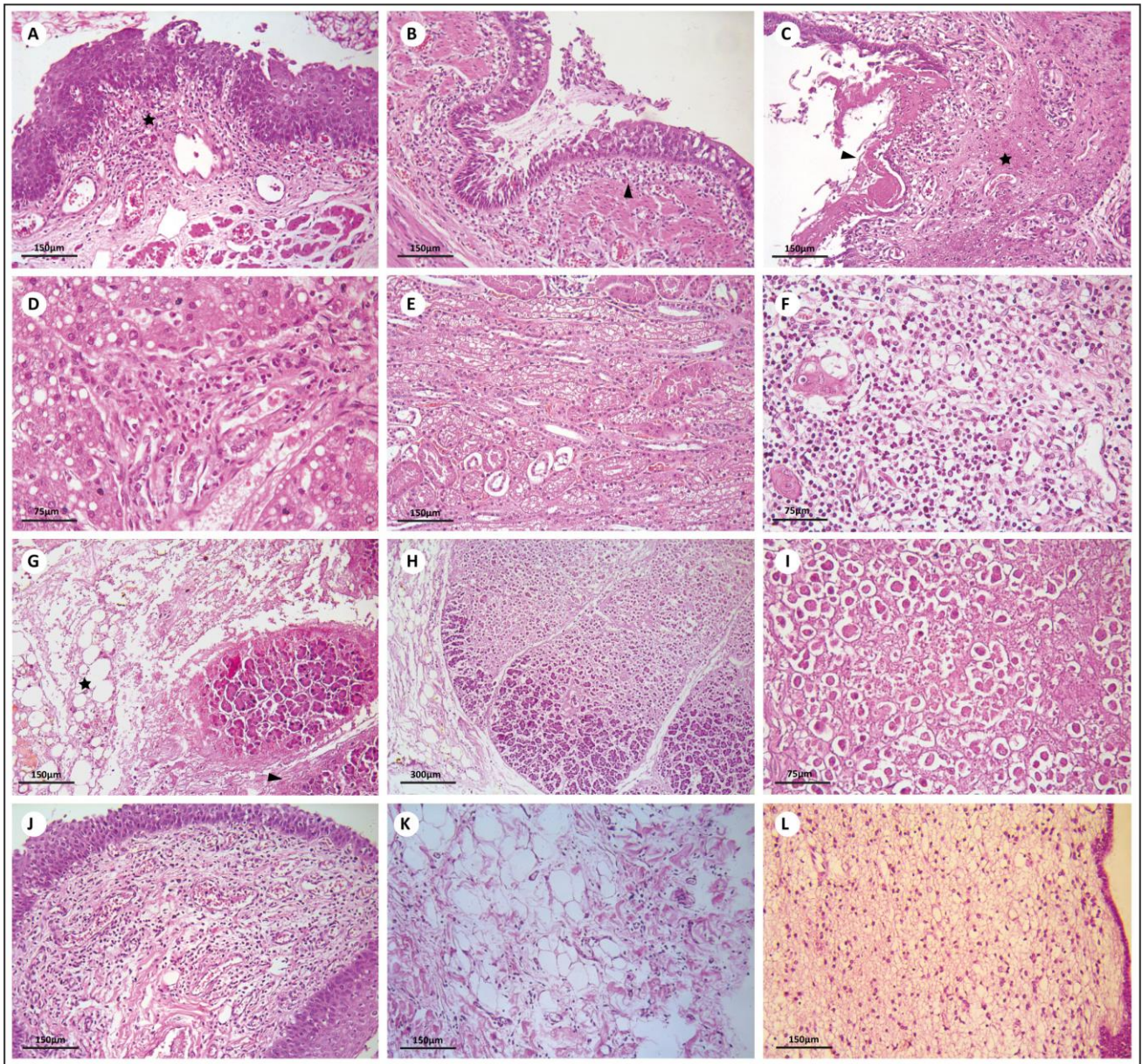
Supplementary Table 1. Morphological findings in various organs.

Organs	Macroscopic Examination	Histopathologic findings
Brain	Marked hypotrophy, edema, hydrocephalus ex vacuo.	Atrophic cerebral cortex, laminar necrosis, spongiosis, gliosis, microgliosis and macrophages. Diffuse white matter edema, microcalcifications (parenchyma and choroid plexus). Mild lymphocytic infiltrate in the cerebral subarachnoid space.
Heart	Normal	Microthrombi in small arteries of left ventricle. Focal mild lymphocytic infiltrate in right ventricle epicardium
Larynx		Laryngitis: moderate lymphocytic inflammatory infiltrate in the mucosa and the submucosa, associated or not with mucosal erosion, necrosis and fibrinonecrotic membrane.
Trachea		Mild lymphocytic infiltrate in some regions of the mucosa and submucosa. Focal squamous metaplasia.
Lungs	Enlarged, with congestion, edema and well demarcated lobules. Pleural effusion.	Pneumonitis: diffuse bronchiolar damage with hyaline membranes and collapsed alveolar spaces, associated with interstitial lymphocytic inflammation, plugs of plasma proteins and cellular debris in bronchiolar lumina, occasionally with macrophages, and lymphoid aggregates in their walls. Pneumocyte type II proliferation in distal respiratory spaces. Congestion, edema, and some foci of hemorrhage and atelectasis. Microthrombi in some small pulmonary arteries. Pleura with mild lymphocytic infiltrate, congestion and edema.
Submandibular salivary glands		Sialoadenitis: focal moderate lymphocytic infiltration in both salivary glands.
Tongue		Severe lymphoid hypoplasia in posterior region and mild interstitial lymphocytic infiltrate around some small salivary glands.
Esophagus		Esophagitis: focal lymphocytic infiltration of the mucosa, along with lymphocyte exocytosis. Regional venular thrombosis.
Stomach		Mild gastritis, some lymphoid aggregates, congestion and foci of superficial hemorrhage of the mucosa.
Intestines		Lymphoid aggregates in the mucosa and submucosa.
Liver	Pale red	Steatosis. Mild lymphocytic infiltration in some portal spaces; occasional recent venular microthrombi.
Pancreas	Dark gray with black areas	Ischemic necrosis of the head, body and tail of the pancreas with hemorrhage. Ischemic steatonecrosis of the regional adipose tissue. Ischemic necrosis of the regional lymph nodes. There was no pancreatitis.

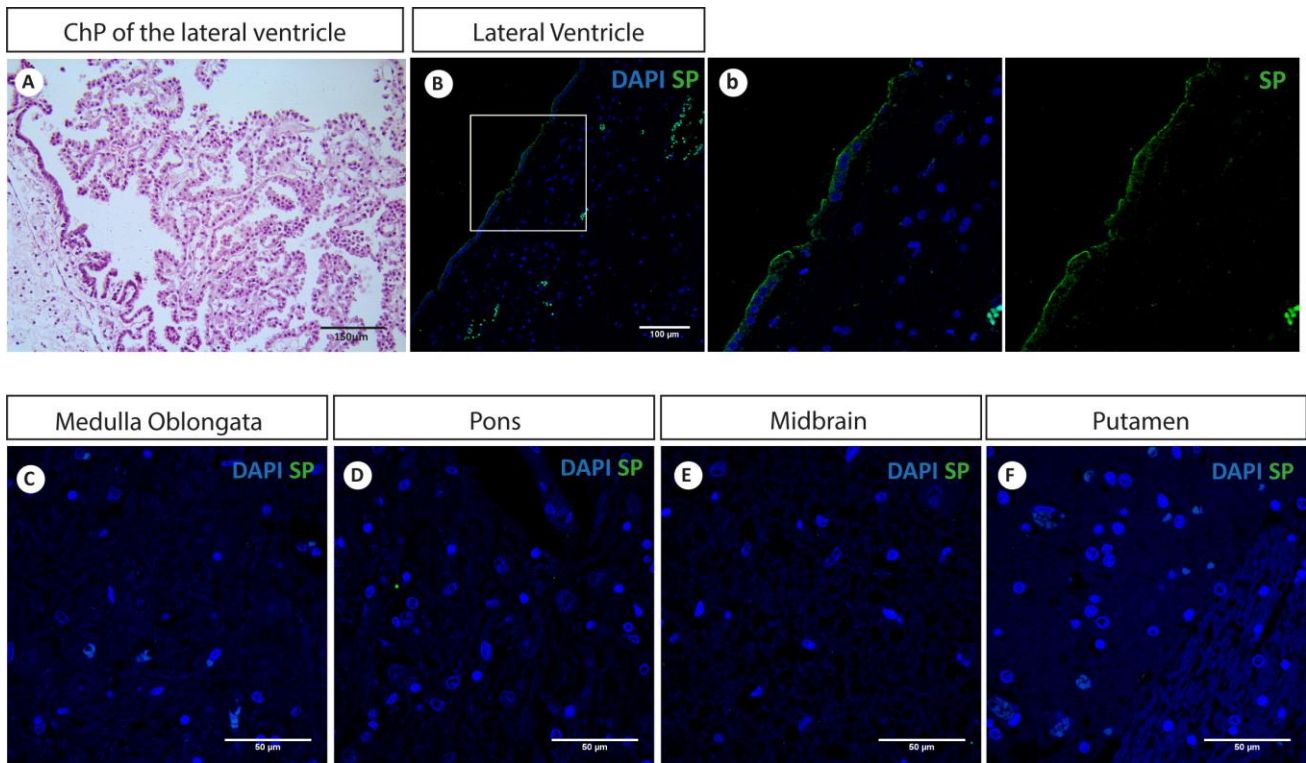
Kidneys	Diffuse osmotic nephrosis secondary to hydroelectrolytic disorders. Some microthrombi in small arteries.
Thymus	Severe diffuse lymphoid hypoplasia.
Vermiform appendix	Severe diffuse lymphoid hypoplasia.
Lymph nodes	Moderate lymphoid hypoplasia.
Spleen	White pulp lacking germinal centers.
Thyroid	Small follicles. Microthrombi in regional small arteries and veins.
Retroperitoneal striated muscle	Focal myositis with lymphocytic inflammatory infiltrate.
Pelvic vein	Focal thrombophlebitis associated with apoptosis of leukocytes in the wall.



Supplementary Figure 1: Light photomicrographs of microthrombosis in multiple organs. (A) Microthrombus in a small pulmonary artery of the left lung, (B) in a small artery in kidney and (C) in left ventricular myocardium. (D) Venous thrombosis in thymus and (E) esophagus. (F) Microthrombus in a small portal vein in the liver (star). (G) Thrombus in veins located adjacent to the thyroid (star). (H) Pelvic thrombophlebitis. Note the adherence of the thrombus (arrowhead) to the endothelium and the venous wall (star) with inflammatory infiltrate. (I) Massive pancreatic ischemic necrosis with extensive hemorrhage (star). H&E.



Supplementary Figure 2: Histological characterization of multiple organs. (A) Esophagus presenting lymphocytic inflammatory infiltrate in the mucosa (star). (B) Tracheitis with lymphocytic inflammatory infiltrate (arrowhead). (C) Laryngitis with necrosis (star) and mucosal erosion covered with eosinophilic and amorphous fibrinonecrotic tissue (arrowhead). (D) Liver steatosis (E) Osmotic nephrosis secondary to hydroelectrolytic disturbances (F) Thymus presenting marked lymphocyte hypoplasia (G)-(H) Ischemic necrosis of the pancreas (arrowhead), along with steatonecrosis of the regional adipose tissue (star). Detail in (I). (J) Posterior region of the tongue presenting marked hypoplasia of the lymphoid tissue (K) Mild pericarditis in right ventricle (L) Periventricular cerebral parenchyma with edema and gliosis. H&E.



Supplementary Figure 3: Photomicrographs of immunofluorescence staining for SP in brain regions. (A) Choroid plexus of the cerebral lateral ventricle (B, b) SARS-CoV-2 infected ependymal cells of the lateral ventricle detected by SP. No SARS-CoV-2 infected cells were detected by SP in (C) medulla oblongata, (D) pons, (E) midbrain, and (F) putamen.